Eur. J. Wood Prod. (2017) 75:43–53
DOI 10.1007/s00107-016-1088-0

ORIGINAL

Ultra-light particleboard: characterization of foam core layer by digital image correlation

Ali Shalbafan[1] · Martin Rhême[2] · Heiko Thoemen[2]

Received: 23 November 2015 / Published online: 26 July 2016
© Springer-Verlag Berlin Heidelberg 2016

Abstract Increasing markets for internet-traded furniture, but also economic concerns are main driving forces to considerably reduce the weight of wood-based furniture panels. Recent research and technological developments have led to an innovative one-step process which simplifies the typical multi-step process for production of foam core panels. Three layered sandwich panels (with particleboard faces and polymeric in situ expanded foam as core layer) can be produced by a one-step process without additional gluing between the face and core layers. As the morphology of the foam and hence its mechanical properties strongly depend on its chemical composition, as well as on the process parameters during expansion, there are no data available, so far, describing the foam of the novel panels. The aim of the proposed project is to determine the elastic properties of in situ expanded foams using 2D digital image correlation. The data can be used later on for the simulation of the elastic behavior of foam core particleboards by means of FEM to describe the short and long term behavior of the panels.

1 Introduction

The future supply with raw materials is of major concern for particleboard producers due to a steadily increasing competition on wooden biomass in the form of wood chips (Mantau et al. 2010). There is currently competition between particleboard manufacturers, pulp mills and energetic usages of wood chips, in the form of fresh fibre material or recovered fibre. Lightweight panels could offer a solution through the development of wood-based foam core panels (sandwich structure) for furniture, which fulfil nearly the same function as particleboard while the amounts of raw material input is significantly reduced (Shalbafan et al. 2012). The customer demand for flat pack furniture is a driving force or an initial reason for the development of lightweight panels. Additionally, the second reason for the lightness seems to be rational from the economic point of view (based on the volume), if the foam materials have the same or even lower prices with regard to the substituted wood materials (Paoletti et al. 2012). Three layered sandwich panels (with particleboard faces and polymeric in situ expanding foam as core layer) can be produced by a one-step process (Luedtke 2011; Shalbafan et al. 2012) without additional gluing between the face and core layers. Such ultra-light particleboard is referred to in this paper as ULPB.

Luedtke (2011) and Shalbafan et al. (2012) used conventional non-bio based polymeric materials for in situ foaming. They have used Expancel microspheres and expandable polystyrene beads as the core layer materials, resulting in different structures and mechanical characteristics of the foamed core layer. Above, the production parameters (press temperature, pressing time and foaming time) controlling the foaming process have a significant influence on the foam structure as well as the physio-mechanical performances of the ULPB, as shown by Shalbafan et al. (2013a,b). Due to the increasing waste and environmental problems of traditional petroleum based foams, further development of the ULPB process towards a fully bio-based lightweight panel is in special focus. Yoon et al. (2016) have developed a polylactic acid (PLA) based

✉ Ali Shalbafan
ali.shalbafan@modares.ac.ir

[1] Department of Wood and Paper Science and Technology, Faculty of Natural Resources and Marine Sciences, Tarbiat Modares University, Noor, Iran

[2] Institute for Materials and Wood Technology, Bern University of Applied Sciences, Bern, Switzerland

source: https://doi.org/10.24451/arbor.5502 | downloaded: 9.1.2022

foam using supercritical CO_2 as blowing agent, fulfilling the requirements for the core layer materials of ULPB mentioned by Shalbafan et al. (2012).

Mechanical characterizations, for example bending properties, of lightweight foam core particleboards with a soft core layer are different from the monolithic wood-based panels and are mainly influenced by the properties of the core material (Mahfuz et al. 2004). In the latter case, only little shear deformation happens during bending, in contrast to the situation in foam core particleboards (Allen 1969). Due to the layered build-up from different materials, the determination of modulus of elasticity (MOE) and strain evaluation (with dial or electrical strain gauge) is not appropriate in conventional three point bending test (Shalbafan et al. 2013b). Strain values measured by pointwise strain gauges (local dial or electrical strain gauges) cannot be necessarily representative of the full picture of foam deformation behavior. Beside of the conventional extensometry, optical strain measurement devices have progressively gained wide acceptance recently for the characterization of the mechanical behavior of different materials (Parsons et al. 2004; Fang et al. 2006; Almeida et al. 2008; Hassel et al. 2009; Godara et al. 2009). Optical measurement apparatus are operated contactless compared to mechanical extensometers which are connected to the test specimen. Such mechanical extensometers led to the local stress concentration raised from the indentation of the specimen. On the other hand, the derivation of the full-field displacement and strain values allows a much better evaluation of the parasitic effects resulting from the experimental set-up using traditional strain gauges (Zhang et al. 2012), making the optical measurement apparatus ideal for polymeric materials.

Generally, optical strain measurement techniques can be categorized into two groups; a) video extensometers which operate with a fixed gauge length measuring the strain between two edges or signs on the test specimen, b) full-field non-contact optical methods (Hild and Roux 2006; Perez et al. 2008). Recently, methods capable of capturing a full-field distribution of the deformations of various materials are more in focus. Two different main groups of full-field non-contact optical methods have been developed and used for full-field surface measurement; (1) interferometric techniques (e.g. holography, speckle and moiré interferometry) and (2) non-interferometric techniques (e.g. grid method and digital image correlation) (Rastogi 2000; Gredia 2004). Briefly, compared with the interferometric optical techniques used for in-plane deformation measurement, the two-dimensional digital image correlation (2D DIC) method has the following advantages; simple experimental setup and specimen preparation, low requirements in measurement environment, wide range of measurement sensitivity and resolution and its applicability to new areas (Hild and Roux 2006). Therefore, two-dimensional digital correlation technique was used in this study for determination of elastic behavior of different foam materials produced during the innovative ULPB process.

Digital image correlation (DIC) technique has been applied to full-field measurement of elastic properties of wood and wood products firstly by Choi et al. (1991) and Zink (1995). However, there have been relatively few studies concerning polymer foam materials using DIC technique. Pierron (2010) has identified the Poisson's ratios with compressive strain of standard low-density (homogeneous) polyurethane foams by using DIC. Fathi et al. (2015) have studied the shear deformations of three common structural core materials to be used for sandwich panels (Balsa wood, PET foam, and cross-linked PVC foam) with the aid of full-field optical DIC analysis. They concluded that full-field strain distributions yielded more comprehensive information about the uniformity of deformation as well as local stress concentrations and initiation of core shear failure. Voiconi et al. (2014) investigated the microstructure and flexural properties of three different rigid PUR foams using DIC technique. They showed that the most significant parameter on mechanical properties of rigid PUR foams is the foam density. Jerabek et al. (2010) have studied the characterization of polypropylene (PP) and PP composite using DIC. They found that the proper strain determination both in the pre- and post-yield regimes is possible. Using different types of polymeric foam in the core layer of ULPB comprising wooden surfaces is under further progress (Yoon et al. 2016). Additionally, the special in situ expanded foaming of core materials leads to the different foam structure (Shalbafan et al. 2012). So, further research is needed particularly on the determination of elastic behavior of different foam materials produced during the innovative ULPB process.

The overall aim of this research is to improve the understanding of the mechanical characteristics of the foam core of the newly developed ULPB by using 2D DIC. The main objective is to determine the elastic characteristics (modulus and Poisson's ratio) of foams using 2D DIC. The samples were loaded in tensile, compression and shear mode and the digital images were taken during the test for further treatment. A comparative analysis of obtained DIC results with reference specimen was also carried out. The following in situ expanded foams have been used as core layer of ULPB; expandable polystyrene (EPS), Expancel microspheres (MS), and a blend of PLA-PMMA (50:50 %).

2 Materials and methods

Foam samples used for testing in this research plan have been produced by two different methods; (a) in-situ expanded foam core particleboards using different

polymeric materials (bio-polymer and synthetic polymer) as core layer, (b) mold production of foam samples as reference.

2.1 Ultra-light particleboard production

2.1.1 Face and core layer materials

Three layered foam core sandwich panels were produced by a one-step process (Shalbafan et al. 2012). Conventional fine wood particles, mainly spruce and pine (≤2 mm), for the face layers were provided from a particleboard mill. The particles were mixed with 12 % urea formaldehyde resin (Kaurit 350, BASF, Germany) based on oven dry mass of the wood particles. Prior to resination, 1 % ammonium sulphate (in case of synthetic polymers as the core layer) or 3 % ammonium persulfate (in case of bio-polymer as the core layer) was added to the resin as hardener. Then, the adhesive was sprayed onto the particle furnish tumbling in a rotating drum-type blender by using a compressed air spray head. The target density and thickness of the surface layers were kept constant with 750 kg/m^3 and 3 mm (each surface layer), respectively.

The heat-sensitive materials for the core layer of ULPB was supplied by different companies; expandable polystyrene from Sunpor (Austria), Expancel microspheres from AkzoNobel (Switzerland), expandable blend of (50:50 % by weight) poly-lactic acids (PLA) with poly methyl methacrylate (PMMA) developed by EPFL and BFH, Switzerland (Yoon et al. 2016). The target density of the foam core and foam layer thickness was kept constant at 100 kg/m^3 and 13 mm for all of the panel variations, respectively. More details about the property of the polymeric core layer materials are listed in Table 1.

2.1.2 Production of the panels

The expandable heat sensitive materials for the core layer were laid manually between the two surfaces after the bottom and before the top surface layer are formed. The three layered mat was then pressed in a computer controlled lab-scale single opening hot press. The temperature of the press plates was set to the level required for the core layer expansion; 160 °C for MS and EPS, and 125 °C for the PLA-PMMA blend.

Since the activation temperature interval for the selected core layer materials is different, the press program to produce foam core panels should be modified for each type of materials. In general, the press cycle for all types of core layer materials was performed in three consecutive stages; pressing phase, foaming phase and stabilization phase. More details about the process program are described in Shalbafan et al. (2012).

To simulate a continuous hot press with a cooling zone for stabilization of the core layer, the pressing schedule will be controlled by initiating the internal cooling of the press plates after approximately 1/3 of the pressing cycle. For each press temperature (125 and 160 °C) and the corresponding program two panel replicates were produced. After panel production, the foam core layer and the testing samples were separated from the wooden surfaces by means of computer numerical control (CNC) cutting machine. From each type of the core layer materials two panels as repetition were produced.

2.1.3 Reference samples

As mentioned earlier, the foam materials were produced and used in a number of different ways. Mold production of foam samples is the closest procedure to the developed one-step process for foam core particleboards. As reference samples, the heat-sensitive PLA-PMMA blend granulates were used in a wooden frame with internal dimensions of 500 × 500 × 13 mm^3 without bottom and surface layers of particleboard. Then, the frame was put on the hot press at a temperature of 125 °C for foaming. The density of the produced foam was also kept constant at 100 kg/m^3.

The experimental samples were taken after mold foam production. The foam samples were tested to determine their elastic properties by using 2D DIC technique. To see the effects of different production processes, the DIC results from molded foam were compared with the corresponding ones obtained from ULPB produced by a one-step process.

Table 1 Property of the polymeric core layer materials

Property	MS	EPS	PLA-PMMA
Particle size	15 µm	0.3–0.8 mm	2–2.5 mm
Particle shape	Spherical	Spherical	Cylinder
Blowing agent	Isobutane	Pentane	Supercritical CO_2
Activation temperature, °C	85	95–115	75
Glass transition temperature, °C	80	103	75

2.2 Principal and concepts of 2D DIC analysis

2.2.1 Specimen preparation

One of the major requirements for DIC is that the surface of the specimen should have a random gray intensity distribution (i.e. the random speckle pattern), which deforms together with the specimen surfaces as a carrier of deformation information. The artificially texture was made by spraying aerosol on the sample surface.

2.2.2 Mechanical testing and test setup

The mechanical tests, tensile, compression and shear tests were performed on a mechanical universal testing machine (Zwick/Roell Z2.5, Germany) with a 2.5 kN load cell. Monotonic loading was performed to measure Young's modulus, shear modulus and Poisson ratio (with loading up to the ultimate strength of the material) of different foam types used for the production of foam core panels. Crosshead displacements were usually set as follows; 0.5 mm/min for tensile tests (MS, EPS, PLA-PMMA), 1.2 mm/min for compression tests (MS, EPS, PLA-PMMA), 3.0 mm/min for shear tests of MS and PLA-PMMA and 1.6 mm/min for EPS samples. The goal was to maintain the time to specimen failure constant at 60 ± 30 s. For the shear test, an Iosioescu device according to ASTM D5379 was used (Magistris and Lennart 2004).

Samples were conditioned for 2 weeks prior to testing at 23 °C and 50 % relative humidity (eight repetitions for each variation). To minimize the effect of temperature variations on the test results, mechanical tests and images acquisition were also performed at the above climate conditions (23 °C and 50 % relative humidity). After foam core panel production, dog-bone samples with a length of 60 mm for tensile and compression tests and V-notched specimens with a length of 76 mm for shear tests were prepared with the help of a CNC machine. Figure 1 shows examples of produced ultra-light panels and the samples geometry with the specified region of interest (ROI). It has to be noted that the surface and bottom layers of foam core layers were also separated using CNC machine.

The Guppy F146B camera (1392 × 1040 resolutions) was placed with its optical axis normal to the specimen surface and imaging the planar sample surface in different loading states onto its sensor plane. To allow for sufficient optical signal detection, two running spotlights with opaque surfaces were also attached around the Guppy camera.

Image acquisition was simultaneously performed through Vimba Viewer program (version 1.1.2 by Allied Vision Technologies Software) and, subsequently, the images were saved in PNG format for further treatments at the running computer. The acquisition frame rates were set

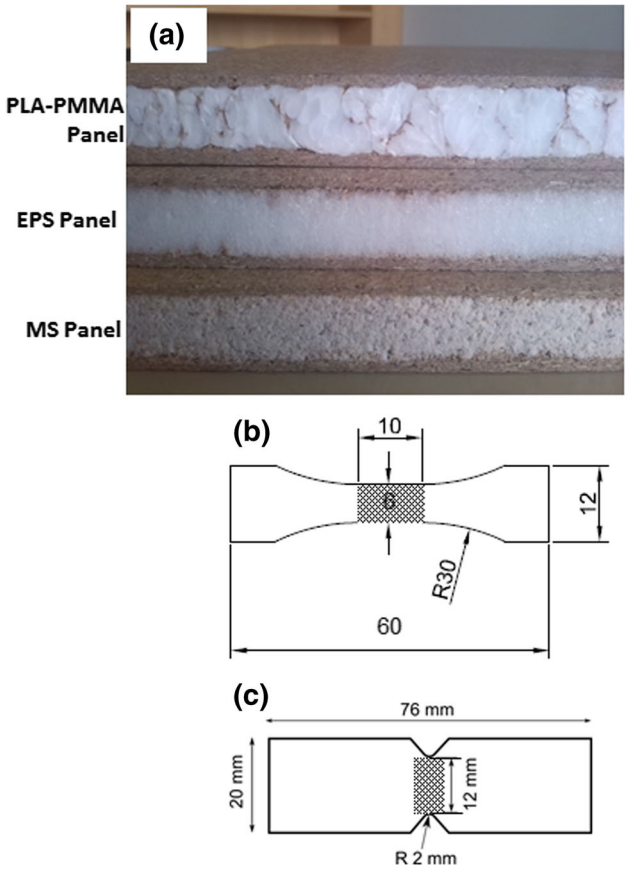

Fig. 1 Produced ultra-light particleboards and derived testing specimens identified with its region of interest (ROI); **a** examples of ULPB, **b** doge-bone samples (sizes in mm) for tensile and compression tests, **c** Iosipescu sample for shear test

at 0.5 for compression tests and 0.6 for tensile and shear tests. Acquisition of analogue inputs from the test machine like force and displacements signal was also done. The camera setup was not connected to the testing machine to avoid vibration effect of the drive system of the test machine on the camera which influences the quality of the test results.

2.2.3 Evaluations of images by 2D DIC

The implementation of 2D DIC comprises several consecutive steps, namely image processing (adjust contrast, gray scale, etc.), initial deformation estimation (initial guesses), displacement measurement, strain field computing, generation of stress–strain curves and finally computing of elastic coefficients. Image processing, displacement measurement and strain field computing were done using MATLAB 2015a program with written code (version 4.2) by Jones (2015). Generation of stress–strain curves and computing of elastic coefficients were performed using Mathematica program.

It should be noted that the 2D DIC analysis usually needs an accurate initial guess of deformation before achieving displacement measurements. For this reason, different techniques for an accurate initial guess were performed. In the present MATLAB code, the results of correlation on reduced images were used as initial guess. Afterwards, full field deformation displacement to sub-pixel accuracy was performed using the desired algorithm. Then, the strains were computed as a numerical differentiation process of the estimated displacement. To improve the accuracy of strain estimation, the computed displacement fields were firstly smoothed by Gaussian distribution of weights with a Kernel size of 11 (control points) and smoothing passes of 3, and then differentiated to strains calculation using cubic algorithm with 16-nodes. Table 2 shows more details of the image correlation and computing displacements and strains in this study.

Determination of the modulus (tensile, compression and shear modulus) and Poisson's ratio in the pre-yield regime and true stress–strain relationships in the post-yield regime is possible using DIC technique (Tscharnuter et al. 2011). The Young's modulus (E) in tensile and compression and shear modulus (G) is the ratio of stress (σ) to corresponding strain (ε) in the elastic regime of the material behavior. The slope of the initial straight segment of the stress–strain diagram is represented as the aforementioned modulus. Poisson's ratio is important for the description of stress and strain states of linear elastic materials. Under simple uniaxial load, Poisson's ratio governs the evolution of the lateral strain. Poisson's ratio (υ) was determined as the negative ratio of the transverse (ε_t) and longitudinal strains (ε_l) in the elastic regime and measured parallel and perpendicular to loading direction, respectively (see Eq. 1);

Table 2 Parameters used for image correlation and computing displacements and strains

Factors	Image correlation		Computation
	Reduced images	Full images	
Image reduction factor	3	–	–
Subset size	35	35	–
Threshold	0.5	0.5	–
Search zone	3	2	–
Repetition of correlation	5	–	–
Kernel size	–	–	11
Number of smoothing passes	–	–	3
Maximum size of contiguous non-correlated points to smooth over	–	–	15
Strain algorithm	–	–	Cubic 16-node

$$\upsilon = -\frac{\varepsilon_t}{\varepsilon_l} \quad (1)$$

2.2.4 *Morphological characterizations of foam cells*

Micromorphology of the foam cells prior to testing and at the failure surfaces was analysed using scanning electron microscope (SEM, HITACHI, TM3030, Germany) at an acceleration voltage of 15 kV. Prepared samples were firstly mounted on stubs and then the surfaces were coated with gold using Mini Sputter Coater (SC7620, Quorum Technologies, UK) at a chamber pressure of 10^{-1} mbar prior to the microscopy observation.

3 Results and discussions

The three principle loading modes tensile, compression and shear, were used for the mechanical characterization of the foams. The elastic parameters of three different foams, EPS, MS and PLA PMMA were characterized in this study.

3.1 Elastic constants for the foams obtained from ULPB

The elastic constants (Young's modulus and Poisson's ratio) can be derived from the strain–stress curves which are presented in Fig. 2a. Young's modulus of three different foams, EPS, PLA-PMMA and MS in two different loading modes (tensile and compression) are presented in Fig. 2b. Young's moduli are quite similar in tension and in compression, but the elastic limit and maximal strength are much more elevated in compression. It was shown that the Young's modulus (in tensile and compression) is the highest for the MS foam both in tensile and compression loading, followed by the PLA-PMMA and EPS foams. The compression Young's modulus in MS foam is nearly doubled compared with the corresponding ones in EPS foam. Besides the density, Young's modulus for the foams are mainly determined by the material properties of the solid cell walls (base materials they are made of) and by their complex microstructure (Gibson and Ashby 1997). MS is a copolymer made of three components; acrylonitrile, methacrylate and acrylates with encapsulating liquid isobutene as blowing agent. EPS foams are made of styrene monomer which is rigid and brittle (Rinde 1970). Mechanical properties of polystyrene are lower compared to those of PLA-PMMA blend due to its origin. Imre et al. (2014) have also shown that PLA-PMMA blend have higher mechanical properties compared to polystyrene.

The foam cell density also influences the foam elasticity. The finer the cell sizes the more cell numbers (foam cell density population) is achieved. Accordingly, the higher

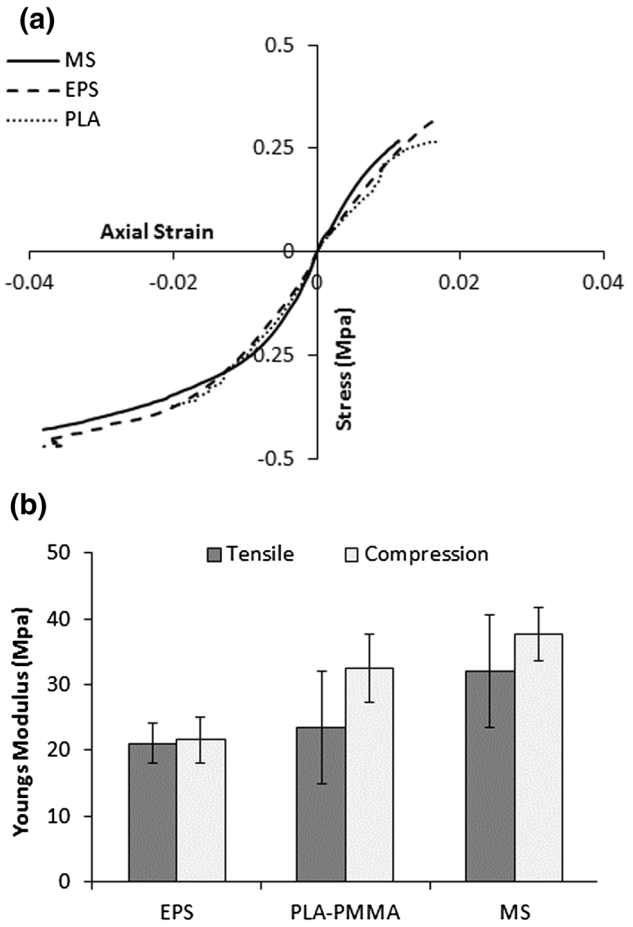

Fig. 2 Strain-stress curves (**a**) and associated Young's modulus (**b**) of three different foams (EPS, PLA-PMMA, MS)

the foam cell density the higher is the elastic modulus of the foams (Hamilton et al. 2013). Electron microscope pictures from the foam cells (EPS, PLA-PMMA and MS) are presented in Fig. 3. Microstructures of the foams show that the finer foam cell sizes and the higher cell numbers were achieved for the MS specimens followed by the PLA-PMMA and EPS, respectively. Similar trend was also observed for the elastic modulus; MS > PLA-PMMA > EPS both in tension and compression loads. Therefore, it can be stated that the predominant factor influencing the Young's modulus for these kinds of foam is their base materials and complex microstructures.

It is also shown in Fig. 2 that the modulus of elasticity in compression loading is higher compared to that of tensile loading, especially for the PLA-PMMA and MS foams. In other words, the tensile and compressive elastic properties are almost identical for the EPS samples while an insignificantly higher Young's modulus in compression was achieved for the PLA-PMMA and MS foams compared to those in tensile. It has to be mentioned that some undesired wood particles from the surface layer entered between the unexpanded granulates of PLA-PMMA and MS foam materials during mat formation. The size of PLA-PMMA granulates was quite big compared to those of EPS granulates (nearly 4 times bigger). During mat forming, several free spaces can be distinguished between the PLA-PMMA granulates; hence, the wood particles during surface layer formation can easily be inserted between granulates. Such wood particles will stay between the foam granulates even after foam expansion. MS cells have extremely small sizes (15 µm) in comparison to those of EPS granulates (0.3-0.8 mm), which makes a homogeneous mat formation technically difficult. Electron microscope pictures from the foam cells (EPS, PLA-PMMA and MS) presented in Fig. 3 show such undesired wood particles in PLA-PMMA and MS foams. These wood particles are caught between the foam granulates which influence the foam beads fusion and accordingly, reduce the elastic modulus in tensile compared with compression. In other words, these wood particles can explain the fact that the samples reached the yield point (Fig. 2a) faster when tested in tensile loading than in compression loading.

The determination of Young's modulus in tensile and compression tests is relatively uncomplicated compared to that of shear modulus which requires much more effort. The modulus of rigidity or shear modulus describes the resistance to deflection of a material caused by shear stresses (Magistris and Lennart 2004). The results for the shear

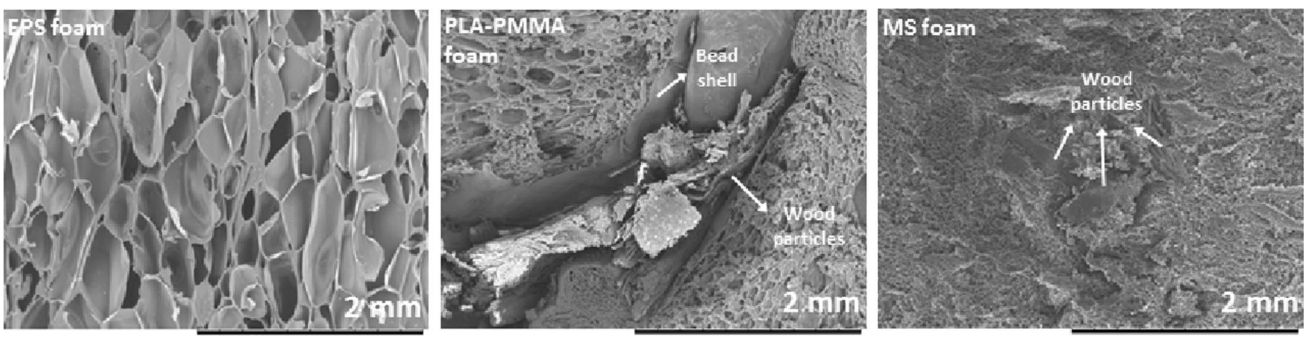

Fig. 3 Microstructure pictures of EPS, PLA-PMMA and MS foams

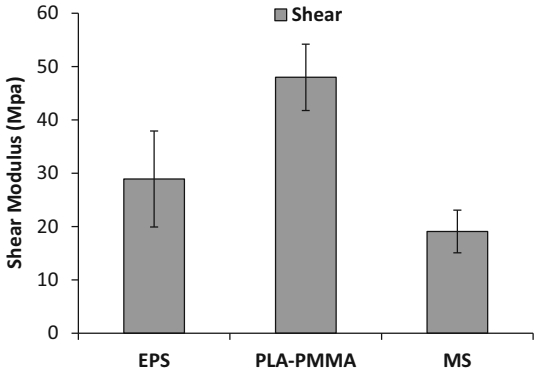

Fig. 4 Shear modulus of three different foams (EPS, PLA-PMMA, MS)

modulus of three different foams, EPS, PLA-PMMA and MS, are presented in Fig. 4. It is visible that the PLA-PMMA foam has significantly higher shear modulus than EPS and MS foams. The modulus of rigidity for the PLA-PMMA blend is nearly 2.5 times higher compared to the MS foam. There are two possible explanations for such trends; effects of cell wall thicknesses and expanded beads fusion. It is logic to say that with a constant foam density (100 kg/m^3), the cell wall thickness is reduced by the increasing cell numbers. The higher the cell numbers the thinner is the cell wall thickness (Shalbafan et al. 2012, 2013b). Due to the huge number of cells and resulting tiny cell sizes in MS, the cell wall thicknesses are very much thinner (<1 μm) than those of PLA-PMMA and EPS foams (>10 μm). The thinner cell wall thicknesses (in MS foam) cannot offer strong resistance to the shear stresses. On the other hand, the PLA-PMMA foam is made of several long polymer beads containing little cells of gas in between. These polymer beads (matrixes) have a shell outside and they are fused together within their shells (Fig. 3). Lots of foam cells are achieved within one single bead of PLA-PMMA due to their bigger bead (granulate) size. Such bead fusions are also achieved to a higher extent for the EPS and MS foams. Close examination of EPS foam shows that homogeneous bead fusion occurred. Actually, the MS foams are made of several individual cells (in micron) fused together with a relatively thin cell wall thickness. MS cell foam was more stressed under shear tests lowering the shear modulus of the foam. Järvelä (1986) and Rossacci and Shivkumar (2003) have also mentioned that the mechanical characterization of the polymeric foams are strongly influenced by the extent of fusion between the polymeric beads. Bead fusion in the foams has a significant effect on the properties of the foam. Shalbafan et al. (2013a, b) have mentioned that the different extent of cell fusion in EPS foam can be achieved in ultra-light particleboard while the process parameters are changing. Such characteristics can also influence the ULPB properties.

The extent of bead fusion can be observed by looking at the fracture surfaces (SEM picture) of the tested samples (Fig. 5). The fracture occurs across the beads (trans-bead fracture) at the EPS and MS foam in different loading scenario (tensile, shear) indicating good bead fusion between both the EPS and MS beads. Actually, a honey-combed cellular structure is observed for both EPS and MS foams. The single EPS and MS beads are hardly distinguishable within the foam structure, since they are almost completely fused together. At the PLA-PMMA foam, the fracture occurs along the beads (inter-bead fracture) showing poor bead fusion. It is worth mentioning that even though inter-bead fracture (poor fusion) happens at the PLA-PMMA foams, such bead fusion strength of the PLA-PMMA beads is still higher in comparison to that of EPS and MS foams (having good bead fusions). This is reflected by the shear modulus presented in Fig. 4. It can be concluded that by improving the bead fusions within the PLA-PMMA foam, obtaining higher shear modulus than the presented value (48 MPa) is also possible. Part f in Fig. 5 shows to some extent scratched parts in the beads surfaces showing that the bead fusion is the predominate factor influencing the shear modulus of the foams. Such scratching parts are not observed during the tensile and compression tests. The cell walls tear in the EPS and MS during the tensile tests and are compressed (cell collapsing) during the compression tests.

The calculated Poisson ratios of the foams within the elastic regime (before yield strength) of the tensile and compression loadings are presented in Fig. 6. It is noteworthy that the Poisson ratios calculated in tensile and compression loading scenarios are mostly identical for each foam types. Higher value is obtained for the EPS samples and the lowest value (nearly half of that) is observed for the PLA-PMMA foam, ranging from 0.42 for the EPS foam to nearly 0.2 for the PLA-PMMA foam. Lower Poisson ratio means that with an axially loaded material, it will not swell/shrink laterally as much.

3.2 Elastic constants for reference PLA-PMMA (RPLA-PMMA) foam

As mentioned earlier and documented in Figs. 3 and 5, some undesired wood particles are inserted between the expanded PLA-PMMA beads during the production of ULPB. These particles result in poorly bonded interfaces between the beads (beads fusion strength), and accordingly, influence the elastic properties of the foam. Reference PLA-PMMA foam (RPLA-PMMA) was produced within a mold in the hot press (without surface and bottom layers of wood particles) having similar density to PLA-PMMA (100 kg/m^3). The reference foam was also tested with different loading functions (tensile, compression, shear)

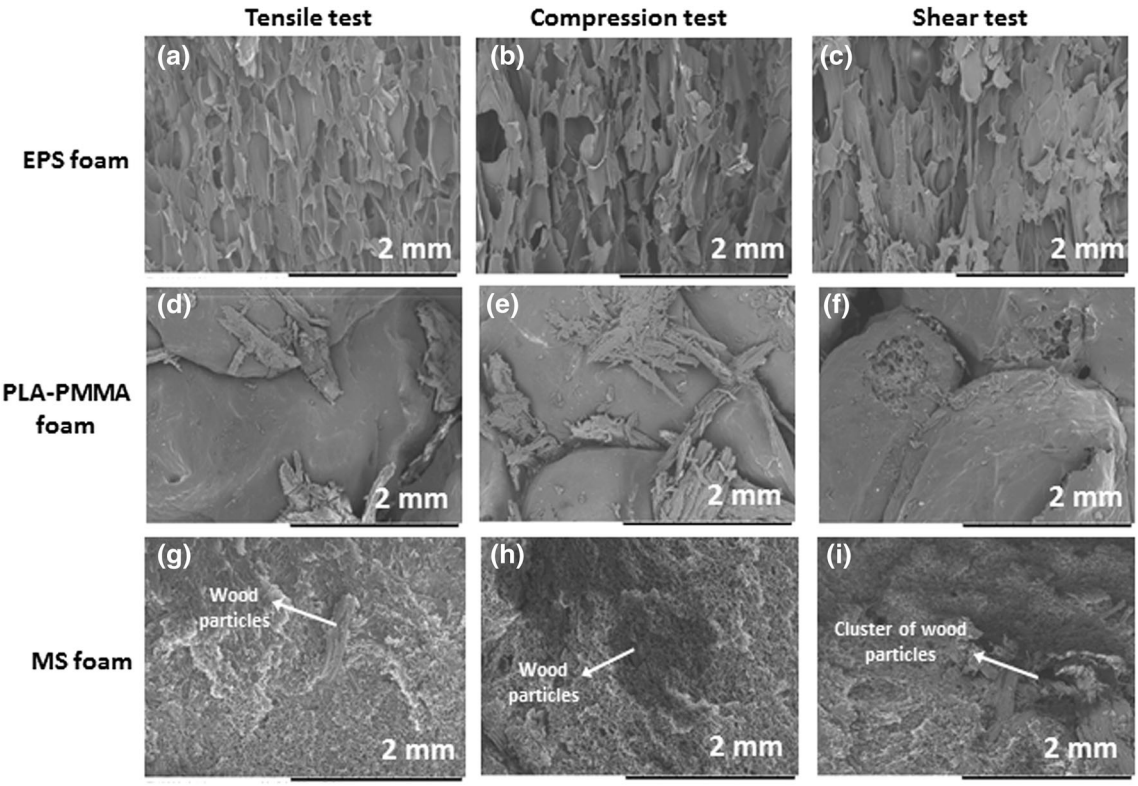

Fig. 5 Fracture surfaces in foams (EPS, PLA-PMMA, MS) showing the extent of bead fusion

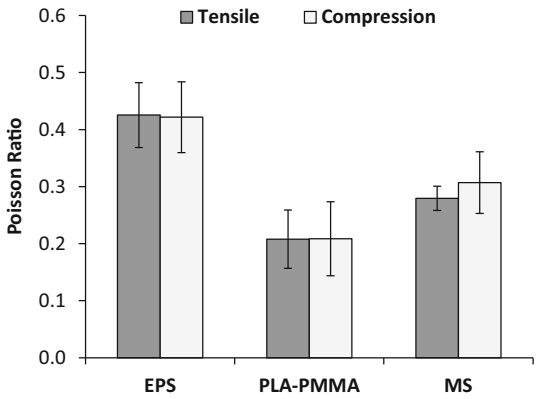

Fig. 6 Poisson ratios of three different foams (EPS, PLA-PMMA, MS)

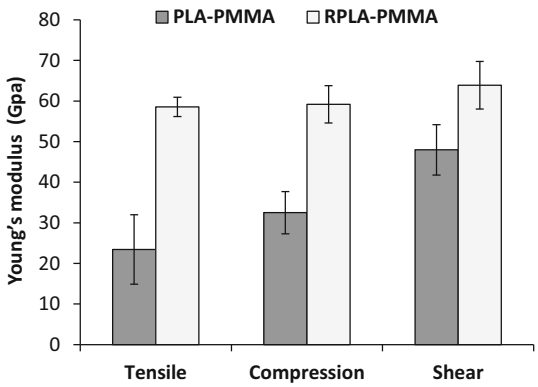

Fig. 7 Young's modulus of PLA-PMMA foam and the reference foam

and its elastic parameters were compared with PLA-PMMA foam and are presented in Fig. 7. It can be seen that the reference foam has quite higher Young's modulus (in tensile and compression) and shear modulus than PLA-PMMA foam obtained from the ULPB. The higher Young's modulus in RPLA-PMMA is due to the reduced cell sizes and accordingly increased cell number of the foam (Fig. 8; part a) (Gibson and Ashby 1997; Hamilton et al. 2013). Young's modulus is almost constant in tensile and compression in RPLA-PMMA which is not the case for the PLA-PMMA. As mentioned before, undesired wood particles between the beads led to the fact that the samples reached faster the yield point while tested in tensile loading than in the compression loading. On the other hand, the loss of elastic linearity in PLA-PMMA foam (in tensile test) is probably due to the fast local damage most likely resulting from the heterogeneities of the foam structure.

The shear modulus for the RPLA-PMMA is likewise enhanced by about 34 percent due to the improved beads fusion in the RPLA-PMMA foam. The enhanced beads

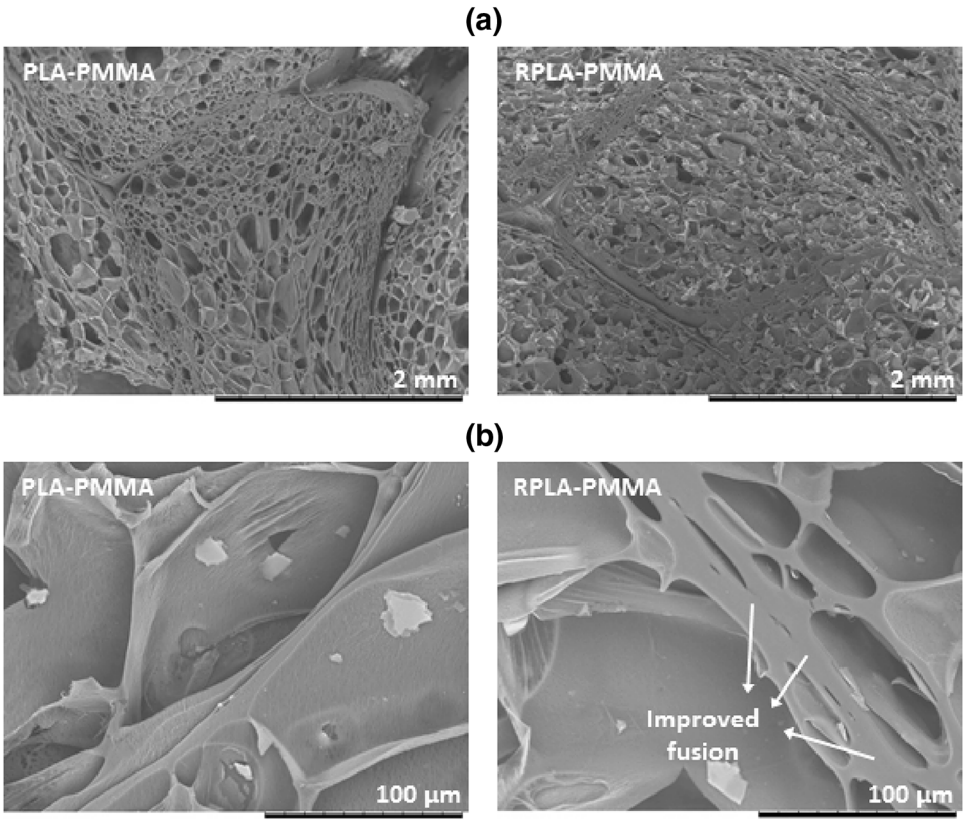

Fig. 8 Bead fusion in PLA-PMMA and RPLA-PMMA foams

fusion is stated in Fig. 8. Bead fusion is improved in some small parts of the beads, while it can still be more improved for the whole beads surfaces. It can be concluded that the improvement of bead fusion in PLA-PMMA foam would have a significant effect on the elastic properties of the foams which can influence the final ULPB properties as well. Shalbafan et al. (2013a) have found that improving the bead fusion in ULPB (made of EPS) has a significant effect on the physical properties of the boards. Reducing the bead size of unexpanded PLA-PMMA can be an option for further research to improve the bead fusion in PLA-PMMA foam. Decreasing the size of expandable PLA-PMMA blend would help to have a more homogeneous mat formation (in the core layer). According to the authors' experiences, the best unexpanded granulate size to produce ULPB is in the range of 0.3–1 mm. Small unexpanded cell sizes (15 µm) for the microspheres (MS) can also lead to the insert of undesired wood particles into the core layer (Luedtke 2011). Furthermore, different process parameters (press temperature, pressing and foaming times) can be used which have significant influence on the microstructure of the foams.

Poisson ratio of PLA-PMMA and RPLA-PMMA are presented in Fig. 9. The Poisson ratio in tensile and compression loading in both types of the foams are also almost identical. An insignificantly higher Poisson ratio for the

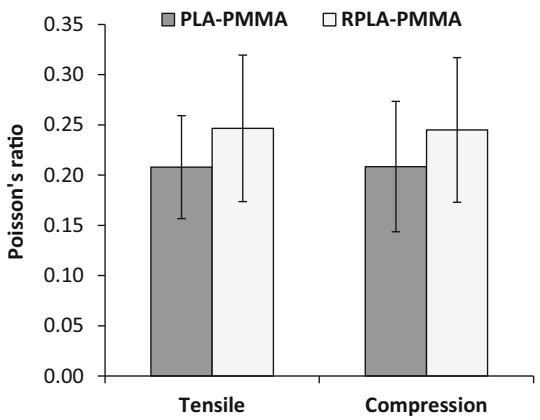

Fig. 9 Poisson ratios of PLA-PMMA foam and the reference foam

RPLA-PMMA was achieved compared to PLA-PMMA foam, which may be due to higher homogeneity and better foam structure in RPLA-PMMA foam.

4 Conclusion

Mechanical characterization of foam part of ULPB (density of 320 kg/m^3) has been performed using DIC technique. It was observed that the behavior of cellular polymer was

dominated by the polymer nature, followed by foam cell sizes and foam beads fusion. It was shown that while the foam cells size has the most significant effect on the Young's modulus of the foam core layers, the cell wall thicknesses and the quality of expanded bead fusion are predominant factors for shear modulus. Foam structures (homogeneity or heterogeneity) are also influencing the differences of Young's modulus in tension and compression tests. An almost identical Young's modulus was achieved for tension and compression tests of homogeneous foam structure (EPS and RPLA-PMMA foam), while the compression modulus is higher for heterogeneous foam structure (PLA-PMMA and MS foams), due to the undesired wood particles in the foams. Photographs of the electron microscope (SEM) also confirmed that the undesired wood particles destructed the homogeneity of the foam which further influenced the elastic constants of the foams. Further research is needed to enhance the foam cell structure of the PLA-PMMA foam through lowering the foam cell sizes and foam beads fusion.

As final conclusion, this research showed that the future of ULPB having bio-based foam materials as the core layer looks bright for the replacement of conventional particleboards.

Acknowledgments Ali Shalbafan would like to acknowledge the Swiss National Science Foundation (SNSF) through the awarded grant (IZK0Z2_162531) to him. The authors are also grateful to Joze Smole, Bern University of Applied Sciences, for panel's preparation. We also thank Sunpor GmbH and BASF for supplying materials.

References

Allen HG (1969) Analysis and design of structural sandwich panels. Pergamon, Oxford

Almeida OD, Lagattu F, Brillaud J (2008) Analysis by a 3D DIC technique of volumetric deformation gradients: application to polypropylene/EPR/talc composites. Compos Part A-APPL S 39(8):1210–1217

Choi D, Thorpe JL, Hanna RB (1991) Image analysis to measure strain in wood and paper. Wood Sci Technol 25(4):251–262

Fang Z, Wang TJ, Li HM (2006) Large tensile deformation behavior of PC/ABS alloy. Polymer 47(14):5174–5181

Fathi A, Keller JH, Altstaedt V (2015) Full-field shear analyses of sandwich core materials using digital image correlation (DIC). Compos Part B-Eng 70:156–166

Gibson LJ, Ashby MF (1997) Cellular solids: structure and properties, 2nd edn. Cambridge University Press, Cambridge

Godara A, Raabe D, Bergmann I, Putz R, Müller U (2009) Influence of additives on the global mechanical behavior and the microscopic strain localization in wood reinforced polypropylene composites during tensile deformation investigated using digital image correlation. Compos Sci Tech 69(2):139–146

Gredia M (2004) The use of full-field measurement methods in composite materials characterization: interest and limitations. Compos Part A-APPL S 35:751–761

Hamilton AR, Thomsen OT, Madaleno LAO, Jensen LR, Rauhe JCM, Pyrz R (2013) Evaluation of the anisotropic mechanical properties of reinforced polyurethane foams. Compos Sci Tech 87:210–217

Hassel BL, Berard P, Modén CS, Berglund LA (2009) The single cube apparatus for shear testing—full-field strain data and finite element analysis of wood in transverse shear. Compos Sci Tech 69(7–8):877–882

Hild F, Roux S (2006) Digital image correlation: from displacement measurement to identification of elastic properties—a review. Strain 42(2):69–80

Imre B, Renner K, Pukanszky B (2014) Interactions, structure and properties in poly(lactic acid)/thermoplastic polymer blends. Express Polym Lett 8(1):2–14

Järvelä P (1986) A method to measure the fusion strength between expanded polystyrene (EPS) beads. J Mater 21(9):3139–3142

Jerabek M, Major Z, Lang RW (2010) Strain determination of polymeric materials using digital image correlation. Polym Test 29:407–416

Jones E (2015) Documentation for Matlab-based DIC Code. University of Illinois at Urbana-Champaign, http://www.mathworks.com

Luedtke L (2011) Entwicklung und Evaluierung eines Konzepts für die kontinuierliche Herstellung von Leichtbauplatten mit polymerbasiertem Kern und Holzwerkstoffdecklagen. Development and evaluation of a concept for the continuous production of lightweight panels comprising a polymer core and wood-based panel facings (in German), Dissertation, Hamburg University, Germany

Magistris FD, Lennart S (2004) Combined shear and compression analysis using the Iosipescu device: analytical and experimental studies of medium density fibreboard. Wood Sci Technol 37(6):509–521

Mahfuz H, Islam MS, Rangari VK, Saha MC, Jeelani S (2004) Response of sandwich composites with nanophased cores under flexural loading. Compos Part B-Eng 35:543–550

Mantau U, Saal U, Prins K, Steierer F, LindnerM Verkerk H, Eggers J, Leek N, Oldenburger J, Asikainen A, Anttila P (2010) Real potential for changes in growth and use of EU forests. Final report of EUwood, Hamburg, Germany

Paoletti S, Spinelli M, Amico M (2012) The European market for RTA furniture. Centre for Industrial Studies, Milano MI, Italy

Parsons E, Boyce MC, Parks DM (2004) An experimental investigation of the large-strain tensile behavior of neat and rubber-toughened polycarbonate. Polymer 45(8):2665–2684

Perez JG, Santana O, Martinez AB, Maspoch MLI (2008) Use of extensometers on essential work of fracture (EWF) tests. Polym Testing 27(4):491–497

Pierron F (2010) Identification of Poisson's ratios of standard and auxetic low density polymeric foams from full-field measurements. J Strain Anal Eng 45(4):233–250

Rastogi PK (2000) Photomechanics: topics in applied physics. Springer, Berlin

Rinde JA (1970) Poisson's ratio for rigid plastic foams. J Appl Poly Sci 14:1913–1926

Rossacci J, Shivkumar S (2003) Influence of EPS bead fusion on pattern degradation and casting formation in the lost foam process. J Mater Sci 38:2321–2330

Shalbafan A, Welling J, Luedtke J (2012) Effect of processing parameters on mechanical properties of lightweight foam core sandwich panels. Wood Mater Sci Eng 7(2):69–75

Shalbafan A, Welling J, Luedtke J (2013a) Effect of processing parameters on physical and structural properties of lightweight foam core sandwich panels. Wood Mater Sci Eng 8(1):1–12

Shalbafan A, Luedtke J, Welling J, Fruehwald A (2013b) Physiomechanical properties of ultra-lightweight foam core particleboards: different core densities. Holzforschung 67(2):69–175

Tscharnuter D, Jerabek M, Major Z, Lang RW (2011) Time-dependent poisson's ratio of polypropylene compounds for various strain histories. Mech Time-Depend Mat 15(1):15–28

Voiconi T, Linul E, Marsavina L, Sadowski T, Knec M (2014) Determination of flexural properties of rigid PUR foams using digital image correlation. Sol St Phen 216:116–121

Yoon Y, Plummer CJG, Thoemen H, Manson JAE (2016) Liquid CO_2 processing of solid polylactide foam precursors. J Cell Plast 52(2):153–174

Zhang S, Dulieu-Barton JM, Fruehmann RK, Thomsen OT (2012) A methodology for obtaining materials properties of polymeric foam at elevated temperatures. Exp Mech 52(1):3–15

Zink A (1995) Image correlation for measuring strain in wood and wood-based composites. Wood Fiber Sci 27(4):346–359